

## Study of Poincaré map associated with the Chua's circuit using interval arithmetic

Zbigniew Galias

Department of Electrical Engineering, University of Mining and Metallurgy  
al. Mickiewicza 30, 30–059 Kraków, Poland  
Phone:+48-12-6172890, Fax:+48-12-6344825, E-mail: galias@agh.edu.pl

### 1. Introduction

The technique of Poincaré map is often used in analysis of continuous-time nonlinear systems. This is a general method which reduces many problems concerning dynamical systems with continuous time to the corresponding problem for dynamical systems with discrete time. In this method one considers the return map which arises on a transversal surface of codimension 1. In this paper, we address the problem if it is feasible to make the analysis via the Poincaré map rigorous. We discuss what kind of problems one could face in an attempt to compute the Poincaré map rigorously.

Rigor is obtained by employing interval arithmetic [3]. Interval computations make it possible to use a computer for calculation of rigorous results, by ensuring that the results obtained enclose the true solution (together with the rounding errors). In this paper, we use boldface to denote intervals, interval vectors and matrices, and the usual math italics to denote point quantities.

The image of a given set under the Poincaré map can be computed rigorously only if the Poincaré map is continuous on this set. Usually the Poincaré map is not defined everywhere. It is not defined for points, trajectories of which never come back to the hyperplane defining the Poincaré map. An example is a point belonging to a stable manifold of an equilibrium of the continuous time system — its trajectory converges to the fixed point and hence never comes back to the Poincaré plane. Even if the Poincaré map is well defined it does not have to be continuous. The Poincaré map is not continuous at points for which the flow is parallel to the Poincaré plane at this point or at the image.

In a close neighborhood of such a discontinuity point rigorous evaluation of the Poincaré map becomes very difficult. Closer to the discontinuity point, the sets which have to be studied become smaller, and the computation time becomes larger. Practically in the regions close to the discontinuity points the rigorous evaluation of the Poincaré map is not feasible. Understanding this problem and knowing the regions, where the Poincaré map is not continuous is the starting point of the rigorous study.

As an example to illustrate these problems we consider the Chua's circuit, a simple third-order dynamical system.

We present methods for rigorous computation of an enclosure of the image of a given set under the Poincaré map. We also show how to compute the Jacobian of the Poincaré map. For the Chua's circuit we find the region, where the Poincaré map is well defined and continuous. In the region, where the Poincaré map can be rigorously evaluated we find all period-2 orbits.

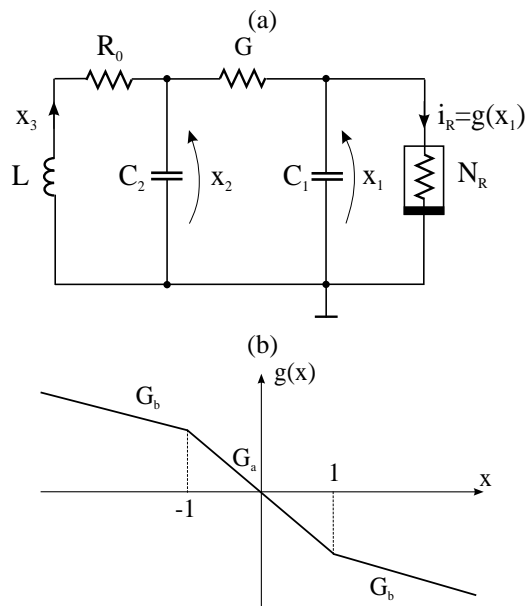


Figure 1: Electronic circuit (a) and characteristics of the nonlinear resistor (b)

### 2. Poincaré map for the Chua's circuit

In this work we present a rigorous study of the Poincaré map associated with the third-order electronic circuit (see Fig. 1(a)), defined by the following set of ordinary differential equations [1]

$$\begin{aligned} C_1 \dot{x}_1 &= G(x_2 - x_1) - g(x_1), \\ C_2 \dot{x}_2 &= G(x_1 - x_2) + x_3, \\ L \dot{x}_3 &= -x_2 - R_0 x_3, \end{aligned} \quad (1)$$

where  $g(z) = G_b z + 0.5(G_a - G_b)(|z + 1| - |z - 1|)$  is a three-segment piecewise-linear function (see Fig. 1(b)).

The system is considered with the following parameter values:  $C_1 = 1$ ,  $C_2 = 9.3515$ ,  $G_a = -3.4429$ ,  $G_b = -2.1849$ ,  $L = 0.06913$ ,  $R = 0.33065$ ,  $R_0 = 0.00036$ , for which chaotic behavior is observed in computer simulations.

The state space  $\mathbb{R}^3$  can be divided into three open regions  $U_1 = \{x \in \mathbb{R}^3: x_1 < -1\}$ ,  $U_2 = \{x: |x_1| < 1\}$  and  $U_3 = \{x: x_1 > 1\}$  separated by planes  $\Sigma_1 = \{x: x_1 = -1\}$  and  $\Sigma_2 = \{x: x_1 = 1\}$ . In the regions  $U_i$  the system is linear, the state equation can be written as:  $\dot{x} = A_i(x - p_i)$ , where  $A_i$  are matrices with real coefficients, and  $p_i$  are vectors, and the solution has the form

$$\varphi(t, x) = e^{A_i t}(x - p_i) + p_i.$$

### 2.1. Generalized Poincaré map

For a standard Poincaré map one considers a single surface of codimension 1. A generalized Poincaré map is defined by a number of surfaces [4]. Let  $\Sigma = \Sigma_1 \cup \Sigma_2$ . The *generalized Poincaré map*  $H: \Sigma \mapsto \Sigma$  is defined as

$$P(x) = \varphi(\tau(x), x), \quad (2)$$

where  $\varphi(t, x)$  is the trajectory of the system based at  $x$ , and  $\tau(x)$  is the time needed for the trajectory  $\varphi(t, x)$  to reach  $\Sigma$ .

The planes separating linear regions are the most natural choice for defining the Poincaré map for piecewise linear systems.

### 2.2. Evaluation of Poincaré map

For rigorous evaluation of  $P$  we use analytical formulas for solutions of linear systems. Let us assume that  $\mathbf{x}$  is a rectangle enclosed in one of the planes  $\Sigma_1, \Sigma_2$ . In the language of interval arithmetic  $\mathbf{x}$  is an interval vector. We assume that trajectories based at  $x \in \mathbf{x}$  enter the linear region where the state equation has the form  $x' = A(x - p)$ . Now we describe the procedure for rigorous computation of the enclosure of the set  $\{P(x): x \in \mathbf{x}\}$ . In the first step of the procedure we find the enclosure of the return time for all points in  $\mathbf{x}$ , i.e. the interval  $\mathbf{t} \supset \{\tau(x): x \in \mathbf{x}\}$ . In order to perform this task we find  $t_1$  such that  $\varphi(s, x) \notin \Sigma$  for all  $x \in \mathbf{x}$  and  $0 < s \leq t_1$ . This ensures that the trajectory based at each point in  $\mathbf{x}$  stays in one linear region for  $s \leq t_1$ . Then we find  $t_2 > t_1$  such that for all  $x \in \mathbf{x}$  the point  $\varphi(t_2, x)$  belongs to another linear region. It follows that the intersection of each trajectory with  $\Sigma$  happens before  $t_2$  and the return time  $\tau(x) \in [t_1, t_2]$  for all  $x \in \mathbf{x}$ . For efficient computations the interval  $\tau = [\tau_1, \tau_2]$  should be as tight as possible. Finally, we use analytic solutions to compute  $\varphi(\tau(\mathbf{x}), \mathbf{x})$ . We find the interval vector

$$\mathbf{R} = e^{A\mathbf{t}}(\mathbf{x} - p) + p. \quad (3)$$

All the computations are done in interval arithmetic and hence  $\mathbf{R} \supset \{\varphi(\tau(x), x): x \in \mathbf{x}\}$ . Finally, the enclosure  $\mathbf{y}$  of  $P(\mathbf{x})$  is computed as the intersection of  $\mathbf{R}$  with  $\Sigma$ , which is equivalent to taking the projection of the interval vector  $\mathbf{R}$  onto the plane  $(x_2, x_3)$ . For the details see [2].

The Jacobian of  $P$  at  $x \in \Sigma$  can be computed using the following formula (compare [4]):

$$P'(x) = \left( I - \frac{A(y - p)e_1^T}{e_1^T A(y - p)} \right) e^{At}, \quad (4)$$

where  $t = \tau(x)$  is the return time,  $y = P(x)$ ,  $e_1 = (1, 0, 0)^T$  and  $I$  is the  $3 \times 3$  identity matrix. The above formula holds if the trajectory  $\varphi(t, x)$  intersects  $\Sigma$  transversally at points  $x$  and  $y$ .

The enclosure of  $P'(\mathbf{x})$  is computed using the formula (4) with the interval quantities  $\mathbf{y}$ ,  $\mathbf{t}$  found in the computation of  $P(\mathbf{x})$ .

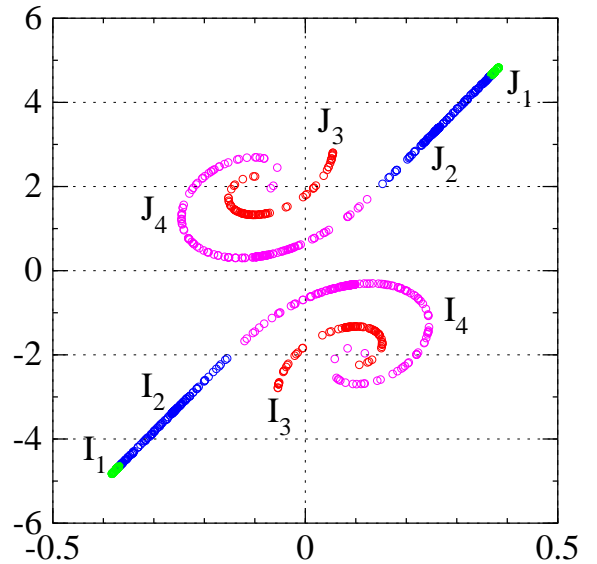


Figure 2: Trajectory of the generalized Poincaré map  $P$ ,  $x_3 > 0 \Rightarrow x \in \Sigma_1$ ,  $x_3 < 0 \Rightarrow x \in \Sigma_2$

### 3. Analysis of the generalized Poincaré map

In Fig. 2 we show a computer generated trajectory of  $P$ . Since the numerically observed attractor intersects the plane  $\Sigma_1$  at points  $x_3 > 0$  and it intersects the plane  $\Sigma_2$  at points  $x_3 < 0$  it is possible to plot the trajectory of the Poincaré map in one figure in spite of the fact that the set  $\Sigma$  consists of two hyperplanes. Now we briefly describe the action of the Poincaré map on points belonging to the attractor for  $x \in \Sigma_2$  (the lower part of the Fig. 2). The intersection of the attractor with the plane  $\Sigma_2$  consists of four components  $I_1, I_2, I_3$  and

$I_4$ . The sets  $I_1$  and  $I_2$  (i.e. the left part of the plot, contained in the region  $\{x_2 < -1.4, x_3 < 0\}$ ) form a line. Trajectories starting here enter the central linear region  $U_2$ . Points  $x \in I_1$  reach the plane  $\Sigma_1$  and their image forms a smaller spiral in the upper halfplane ( $P(x) \in J_3$ ). Points  $x \in I_2$  return back to the  $\Sigma_2$  plane and their image forms the larger spiral in the lower halfplane ( $P(x) \in I_4$ ). The right part of the plot is composed of two spirals ( $I_3$  and  $I_4$ ). Trajectories starting here enter the linear region  $U_3$  and return back to  $\Sigma_2$ . Their images form the left part of the plot ( $P(x) \in I_1 \cup I_2$  for  $x \in I_3 \cup I_4$ ).

These transitions can be written in the following way  $I_1 \rightarrow J_3, I_2 \rightarrow I_4, I_3, I_4 \rightarrow I_1 \cup I_2$ . Similarly for the plane  $\Sigma_1$  we have:  $J_1 \rightarrow I_3, J_2 \rightarrow J_4, J_3, J_4 \rightarrow J_1 \cup J_2$ .

From the discussion presented above one can easily identify one region in  $\Sigma_2$ , where the rigorous evaluation of the Poincaré map may be difficult or even impossible. The border between the sets  $I_1$  and  $I_2$  is composed of points for which trajectory intersects  $\Sigma_1$  tangentially. At this border rigorous computation using the methods given above is not possible. Observe that the set  $I_1 \cup I_2$  is connected, and hence one can expect that there are points belonging to the attractor at which rigorous analysis is not possible.

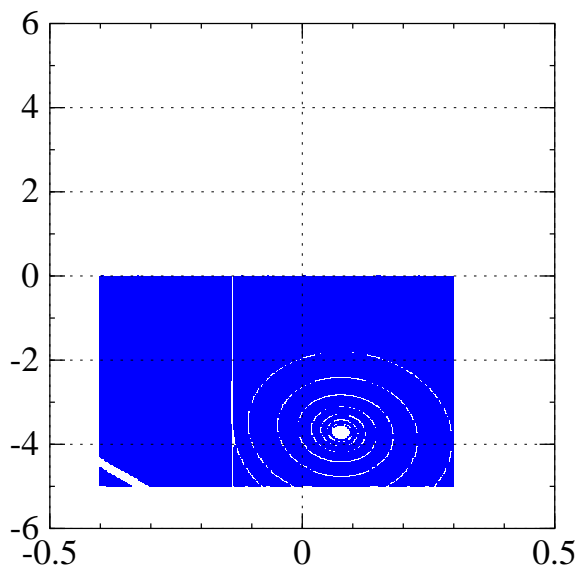


Figure 3: Set  $V$  — boxes belonging to the rectangle  $[-0.4, 0.3] \times [-5, 0]$  for which the Poincaré map can be computed rigorously

For the Chua's circuit we start the analysis by finding the subsets of  $\Sigma$ , where the Poincaré map can be rigorously evaluated. Since the vector field defining the Chua's circuit is symmetric with respect to the origin it is sufficient to make the analysis for  $\Sigma_2$ . The rectangle  $\{1\} \times [-0.4, 0.3] \times [-5, 0] \subset \Sigma_2$  contains the numerically observed attractor

(compare Fig. 2). This rectangle is covered by boxes of the form  $\{1\} \times [i/400, (i+1)/400] \times [j/40, (j+1)/40]$ . The boxes for which we were able to compute the image under the Poincaré map are plotted in Fig. 3. We denote this set by  $V$ .

The set of boxes for which the computation was unsuccessful is composed of three parts. Vertical line of boxes contains a set of points in the state space where the vector field is parallel to the plane  $\Sigma_2$  ( $\dot{x}_1 = 0$  and  $x_1 = 1$ , i.e.,  $x_2 = 1 + G_a/G \approx -0.1383$ ).

The part in the lower left corner contains a curve in  $\Sigma_2$  of points  $x$  for which the intersection of the trajectory with the plane  $\Sigma_1$  is not transversal. This curve separates points for which  $P(x) \in \Sigma_2$ , from points for which  $P(x) \in \Sigma_1$ . Clearly the Poincaré map is not continuous on the curve and if a box contains a point from this curve evaluation of the Poincaré map on this box is not possible.

The third part is the spiral on the right hand side. It contains points for which the intersection of the trajectory with the plane  $\Sigma_2$  at  $P(x)$  is not transversal (the spiral is the preimage of the vertical line in  $\Sigma_2$  for which  $\dot{x}_1 = 0$ ). The region in the center of the spiral contains the intersection of the stable manifold of the equilibrium enclosed in the region  $U_3$  with the plane  $\Sigma_2$ . The Poincaré map is not defined at this point. Rigorous evaluation of the Poincaré map in the neighborhood of this point is difficult since trajectories starting close to this point spend long time in the neighborhood of the unstable equilibrium.

One can see that for the Chua's circuit all types of the phenomena leading to problems with rigorous evaluation of the Poincaré map occur.

The first part, i.e. the vertical line is not very important for the analysis, since the attractor does not intersect this line. Unfortunately, the other two parts intersect the numerically observed attractor and this fact limits the completeness of the results which can be obtained by studying the system rigorously, even if we limit the analysis to a neighborhood of the numerically observed attractor.

### 3.1. Periodic orbits

In the second step of our study we would like to find all short cycles of the Poincaré map. It is well known that interval Newton method and bisection technique can be successfully used for finding all low period cycles of discrete time systems. Since the Poincaré map is not continuous everywhere, we cannot find all its short periodic orbits. It should however be possible to find all periodic orbits enclosed in the region for which the Poincaré map can be evaluated.

From the definition of generalized Poincaré map it follows that all periodic points must have an even period.

Using the generalized bisection and the interval Newton method we have found all period-2 orbits, i.e. the shortest orbits possible of the generalized Poincaré map enclosed in the set  $V$ . We have proved that there is only one

period-2 orbit in this region. The periodic point belongs to the interval vector  $(-0.33311448212, -0.33311448210) \times (-4.2398951156, -4.2398951154)$ . We have also shown that the length of the corresponding periodic orbit of the continuous time system belongs to the interval  $(7.380584397, 7.380584399)$ .

Symmetrically, there is another period-2 orbit intersecting the plane  $\Sigma_1$ .

Further analysis of the Poincaré map on the entire set  $V$  is very time consuming. We have not managed to find all periodic orbits of period 4. In order to reduce the time complexity of the problem we limit our investigations to the region containing the numerically observed attractor. To this end we cover the numerically generated trajectory of the Poincaré map by 15346 boxes of size  $0.001 \times 0.01$  (see Fig. 4). For 204 boxes in 16 connected components the computation of the Poincaré map was unsuccessful. These boxes are located close to the intersection of the computer generated attractor with the set of points on  $\Sigma$  where the Poincaré map is not defined or is not continuous. The set  $W$  is defined as the union of boxes, for which computation was successful.

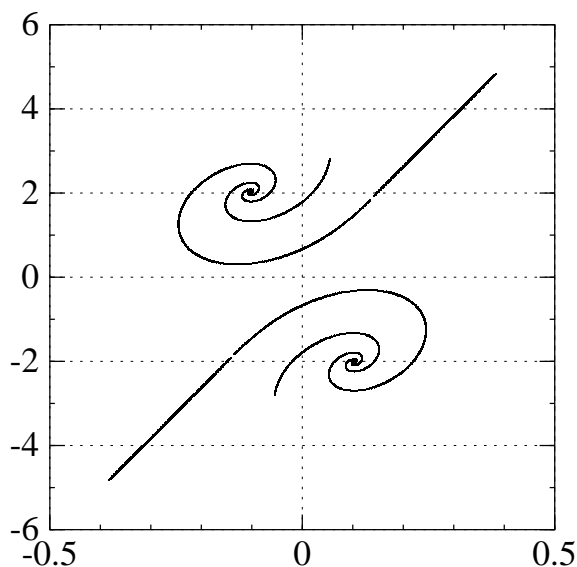


Figure 4: Covering of the computer generated trajectory of the Poincaré map by boxes

In Fig. 5 we show the invariant part of the set  $W$ . It is found by removing boxes which has empty intersection with  $P(W)$  and boxes whose image has empty intersection with  $W$ . The procedure is continued until no boxes can be removed.

The number of boxes obtained in this way is significantly smaller than for the set  $V$ . Such reduction makes it possible to find all cycles for larger period. The results on this study will be reported elsewhere.

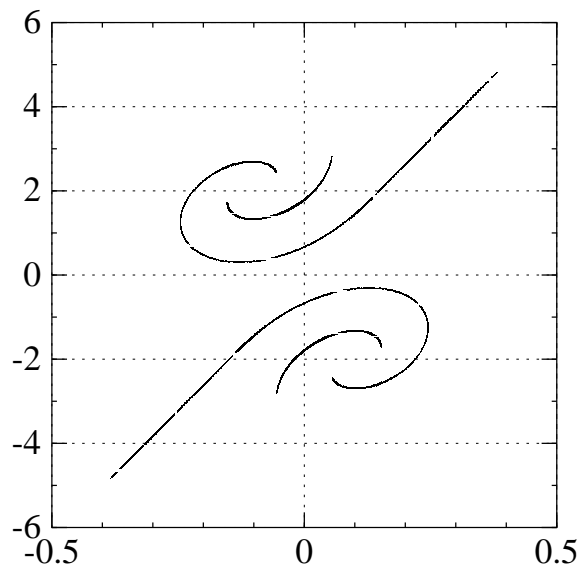


Figure 5: Invariant part

#### 4. Conclusions

In this paper we have studied a possibility of rigorous investigation of the Poincaré map associated with the Chua's circuit. We have identified regions where rigorous evaluation of the Poincaré map is not possible. Since these regions intersect the numerically observed attractor it is plausible to believe that full analysis of the Chua's circuit may be not possible. We have proved that in the region where the numerical procedure succeeds in computation of the Poincaré map there is only one pair of symmetric period-2 orbits.

#### Acknowledgments

This research was supported by the University of Mining and Metallurgy, Kraków, grant no. 10.10.120.133.

#### References

- [1] L.O. Chua. Global unfolding of Chua's circuit. *IEICE Trans. Fundamentals*, E76-A(5):704–734, 1993.
- [2] Z. Galias. Positive topological entropy of Chua's circuit: A computer assisted proof. *Int. J. Bifurcation and Chaos*, 7(2):331–349, 1997.
- [3] R.E. Moore. *Methods and applications of interval analysis*. SIAM, Philadelphia, 1979.
- [4] T.S. Parker and L.O. Chua. *Practical numerical algorithms for chaotic systems*. Springer Verlag, New York, 1989.